NIH Public Access
Author Manuscript
Free Radic Biol Med. Author manuscript; available in PMC 2013 January 01.

Published in final edited form as:
Free Radic Biol Med. 2012 January 1; 52(1): 173–181. doi:10.1016/j.freeradbiomed.2011.10.442.

Manganese superoxide dismutase inhibits neointima formation through attenuation of migration and proliferation of vascular smooth muscle cells

Jia-Ning Wang[a,b], **Ning Shi**[a], and **Shi-You Chen**[a,*]

[a]Department of Physiology & Pharmacology, University of Georgia, Athens, GA 30602, USA

[b]Institute of Clinical Medicine and Department of Cardiology, Renmin Hospital, Hubei University of Medicine, Shiyan, Hubei 442000, China

Abstract

Superoxide anion is elevated during neointima development and is essential for neointimal vascular smooth muscle cell (VSMC) proliferation. However, little is known about the role of manganese superoxide dismutase (MnSOD, SOD2) in the neointima formation following vascular injury. SOD2 in the mitochondria plays an important role in cellular defense against oxidative damage. Because of its subcellular localization, SOD2 is considered the first line of defense against oxidative stress and plays a central role in metabolizing superoxide. Because mitochondria are the most important sources of superoxide anion, we speculated that SOD2 may have therapeutic benefits in preventing vascular remodeling. In this study, we used a rat carotid artery balloon-injury model and an adenoviral gene delivery approach to test the hypothesis that SOD2 suppresses vascular lesion formation. SOD2 was activated along with the progression of neointima formation in balloon-injured rat carotid arteries. Depletion of SOD2 by RNA interference markedly promoted the lesion formation, whereas SOD2 overexpression suppressed the injury-induced neointima formation via attenuation of migration and proliferation of VSMCs. SOD2 exerts its inhibitory effect on VSMC migration induced by angiotensin II by scavenging superoxide anion and suppressing the phosphorylation of Akt. Our data indicate that SOD2 is a negative modulator of vascular lesion formation after injury. Therefore, SOD2 augmentation may be a promising therapeutic strategy for the prevention of lesion formation in proliferative vascular diseases such as restenosis.

Keywords

Manganese superoxide dismutase; Oxidative stress; Neointima; Migration; Proliferation; Vascular smooth muscle cells; Signal transduction; Free radicals

Drug-eluting stents (DESs) are now routinely used for occlusive atherosclerotic coronary lesions to reduce restenosis. However, DESs have been associated with a higher frequency of late stent thrombosis or reinfarction due to a delayed reendothelialization of the vessel wall after stenting. As a result, DESs require prolonged periods of dual anti-platelet therapy [1,2]. It is clear that restenosis continues to be an intractable challenge in the field of cardiovascular therapeutics. Complete understanding of the molecular mechanisms controlling the process of restenosis, therefore, is essential for solving this medical problem.

© 2011 Elsevier Inc. All rights reserved.

*Corresponding author. Fax: +1 706 5423015. sc229@uga.edu (S.-Y. Chen).

NIH-PA Author Manuscript
NIH-PA Author Manuscript
NIH-PA Author Manuscript

NIH-PA Author Manuscript

NIH-PA Author Manuscript

NIH-PA Author Manuscript

Migration and proliferation of vascular smooth muscle cells (VSMCs) play a pivotal role in neointima growth after angioplasty or stenting [3]. Excessive neointima growth is a major cause of restenosis after percutaneous coronary intervention, significantly narrowing the vessel's lumen [4]. Studies have shown that superoxide anion ($O_2^{\bullet -}$) is elevated in the developing neointima and essential for neointimal VSMC proliferation [5]. $O_2^{\bullet -}$ stimulates transcriptional activities of Fos family genes and phosphorylation of mitogen-activated protein kinases [6] and regulates protein phosphatase activity [7] and nuclear factor-κB signaling in VSMCs [8]. Fortunately, natural defense systems against oxidative stress are present in blood vessels. In the blood vessel wall, there are three isoforms of superoxide dismutase (SOD): cytosolic or copper–zinc SOD (CuZn-SOD, SOD1), manganese SOD (Mn-SOD, SOD2) localized in mitochondria, and an extracellular form of CuZn-SOD (EC-SOD, SOD3) bound in cell membranes through its heparin-binding domain and located extracellularly [9–11]. Under normal conditions, the mitochondrial electron transport chain is a major source of superoxide, converting up to 5% of O_2 molecules to superoxide. Because of its subcellular localization, SOD2 is considered the first line of defense against oxidative stress and plays a central role in metabolizing superoxide [11].

A large body of experimental studies have shown that SOD1 or SOD3 gene transfer inhibits neointima formation and promotes endothelial recovery in rabbit atherosclerotic or balloon-denuded aorta [12–14]. However, little is currently known about the role of SOD2 in neointima formation after vascular injury. It is also unknown if SOD2 regulates SMC proliferation or migration.

Because mitochondria are the most important sources of $O_2^{\bullet -}$ [15], determination of the role of SOD2 in neointima formation is clearly important for developing therapeutics to effectively prevent $O_2^{\bullet -}$-induced vascular remodeling. In this study, we used a well-defined rat carotid artery balloon-injury model and an adenoviral gene delivery approach to test the hypothesis that SOD2 may suppress lesion formation after vascular injury. We found that SOD2 was activated in the progression of neointima formation in balloon-injured arteries. Knockdown of SOD2 markedly promoted the lesion formation, whereas SOD2 overexpression suppressed the injury-induced neointima formation by attenuating VSMC migration and proliferation. SOD2 exerts its inhibitory effect on VSMC migration by scavenging $O_2^{\bullet -}$ and suppressing the phosphorylation of Akt. Our data indicate that overexpression of SOD2 may be a promising therapeutic strategy for the prevention of lesion formation in proliferative vascular diseases such as restenosis.

Materials and methods

Animals

Male Sprague–Dawley rats weighing 450–500 g were purchased from Harlan. All rats were housed under conventional conditions in animal care facilities. All animals received humane care in compliance with the *Principles of Laboratory Animal Care* formulated by the National Society for Medical Research and the *Guide for the Care and Use of Laboratory Animals*. All animal experiments were approved by the Animal Care and Use Committee of the University of Georgia.

Cell culture

VSMCs were isolated by autogrowth of explant culture from rat thoracic aortas as described previously [16]. Briefly, rat thoracic aortas were removed and washed with Dulbecco's modified Eagle's medium (DMEM). Media were carefully dissected from the vessels and cut into pieces (<1 mm^3). Tissue pieces were then explanted onto a fibronectin-coated cell culture flask. To get a firm attachment of tissue pieces, the flask was incubated upside-down

NIH-PA Author Manuscript

NIH-PA Author Manuscript

NIH-PA Author Manuscript

for 1 h and then DMEM supplemented with 20% fetal bovine serum (FBS), penicillin, and streptomycin was slowly added. Cells were allowed to autogrow for 2 weeks and then passaged until enough cells were obtained. VSMCs were maintained in DMEM supplemented with 10% FBS, penicillin, and streptomycin at 37 °C in a humidified atmosphere of 5% CO_2. VSMCs were characterized by the expression of smooth muscle α-actin and SM22α.

Reverse transcriptase polymerase chain reaction (PCR) for cloning SOD2 cDNA

RNA was isolated from cultured VSMCs using Nucleospin RNA II 50 Preps (Fisher Scientific) according to the manufacturer's instructions. Single-stranded cDNA was synthesized from 1 μg of total RNA using an iScript Select cDNA synthesis kit (Bio-Rad). PCR of SOD2 cDNA was carried out. The sequences of PCR primers for SOD2 were forward 5′-ACGCCCGGGCCTCGAGACCATGTTGTGTCGGGCGGCGTGCAGC-3′ (43 bp) and reverse 5′-CCTTGTAGTCCTCGAGCTTCTTGCAAACTATGTATCTTTGGC T-3′ (43 bp), which generated a 669-bp PCR product used for fusion with the shuttle vector. The SOD2 PCR products were analyzed by aga-rose gel electrophoresis to verify the expected size and subsequently confirmed by sequencing [17].

Construction of adenoviral SOD2 expression or short-hairpin (sh) RNA vectors

The SOD2 cDNA generated as described above was subcloned into the XhoI site of pShuttele-IRES-hrGFP-1 (Agilent) using the In-Fusion Advantage PCR cloning kit (Clontech) according to the manufacturer's instructions and was verified by sequencing. The sequences encoding rat SOD2 shRNA were as follows: top strand, 5′-CGCGTCGGATTGATGTGTGGGAGCACGCTTATTCAAGAGATAAGC GTGCTCCCACACATCAATCCTTTTTTCCAAA-3′ (76 bp); bottom strand, 5′-AGCTTTTGGAAAAAAGGATTGATGTGTGGGAGCACGCTTATCTCTTGAAT AAGCGTGCTCCCACACATCAATCCGA-3′ (76 bp). The two strands were annealed and ligated into MluI/HindIII-digested pRNAT-H1.1/Adeno (Cat. No. SD1219; Genscript Corp.). Recombinant adenoviral vectors were produced by homologous recombination within AD-1 competent cells according to the manufacturer's instructions for the AdEasy XL system (Agilent). The resultant recombinant vectors pAd-SOD2 and pAd-shSOD2 were transfected into AD-293 cells to package respectively Ad-SOD2 or Ad-shSOD2 viral particles. The adenovirus was purified with cesium chloride gradient density ultracentrifugation and dialyzed in dialysis buffer (135 mM NaCl, 10 mM Tris–HCl, pH 7.5, 1 mM $MgCl_2$, 10% glycerol). The green fluorescent protein (GFP) adenovirus (Ad-GFP) used as a control in this study was described previously [16].

Rat carotid artery injury model and adenoviral gene transfer

The rat carotid artery balloon-injury model was based on a model described by Clowes et al. [18]. Briefly, rats were anesthetized by an intraperitoneal injection of ketamine (80 mg/kg) and xylazine (5 mg/kg). A 2 F Fogarty arterial embolectomy balloon catheter (Baxter Edwards Healthcare, Irvine, CA, USA) was introduced through the left external carotid artery and advanced 4 cm toward the thoracic aorta. The balloon was inflated with 20 μl of 0.9% sodium chloride (saline) and then withdrawn through the common carotid artery to the carotid bifurcation with constant rotation between the fingers during denudation of the endothelia. This procedure was repeated two more times to ensure complete endothelial denudation. Heparin (200 u/kg) was then intraperitoneally injected to prevent thrombus formation. The protocol used for introducing adenovirus into rat balloon-injured carotid artery has been described previously [19]. The injured carotid artery was washed with saline and incubated with 100 μl of saline or adenovirus (5×10^9 pfu) expressing GFP, SOD2, or SOD2 shRNA for 20 min. Fourteen days later, the balloon-injured artery segment from the proximal edge of the omohyoid muscle to the carotid bifurcation was perfused with saline

NIH-PA Author Manuscript

NIH-PA Author Manuscript

NIH-PA Author Manuscript

and excised. The tissue was then fixed with 4% paraformaldehyde and paraffin-embedded. Subsequent morphometric analyses were performed in a double-blinded manner.

Histomorphometric analysis and immunohistochemistry staining (IHC)

Vessel segments were cut by serial sectioning (5 μm), and 10 sections that were evenly distributed in the vessel segment were collected for analysis. The sections were stained with modified he-matoxylin and eosin (H&E) or Elastica van Gieson staining. Cross-sectional images were captured with a Nikon microscope and a Nikon camera (Nikon America). The circumferences of the lumen, internal elastic lamina, and external elastic lamina were measured by image analysis (ImagePlus Software) [20,21]. For immunohisto-chemistry staining, sections were rehydrated, blocked with 5% goat serum, permeabilized with 0.01% Triton X-100 in PBS, and incubated with SOD2 antibody overnight at 4 °C. The sections were counterstained with hematoxylin.

Western blot analysis

VSMCs or rat carotid arteries were homogenized in homogenization buffer (50 mmol/L Tris–HCl, pH 7.5, 150 mmol/L NaCl, 1% SDS, protease inhibitor cocktail (Sigma–Aldrich)). After removal of cell or tissue debris by centrifugation, 20 μg of proteins was separated on 10% SDS–PAGE and transferred to an Immobilon transfer membrane (Millipore). Antibodies against SOD2, Akt, phospho-Akt (Ser473), and α-tubulin were used for immunoblotting followed by horseradish peroxidase (HRP)-conjugated secondary antibodies. All samples were loaded equally for each gel based on protein concentration. Western blots were performed as described previously [22].

Wound healing assay

Migration evaluation was performed with a wound healing assay [23,24]. This was carried out according to the manufacturer's manual for the CytoSelect 24-well wound healing assay (Cell Biolabs). In brief, 24-well cell culture plates were coated with fibronectin, and wound healing inserts (0.9 mm in width) were put into the wells with the inserts aligned in the same direction and in firm contact with the bottom of the wells. VSMCs infected with Ad-GFP or Ad-SOD2 or Ad-shSOD2 (250 μl) were added to either side of the open ends at the top of the insert and incubated overnight to form a monolayer. Then the inserts were removed to begin the wound healing assay for 48 h. For each well, pictures were taken on a dissection microscope at a magnification of 40×. Cell migration was quantified by blind measurement of the migrated distance.

Cell proliferation

Cell proliferation was evaluated with the MTT assay according to the commercial manufacturer's instructions for the TACS MTT cell proliferation assay (Cat. No. 4890-25-K; Trevigen) [25]. The optical density at 570 nm was measured and compared.

Determining intracellular superoxide anion production

To determine intracellular $O_2^{\bullet-}$ production in VSMCs, we used dihydroethidium (DHE; Invitrogen, Carlsbad, CA, USA) [26]. In this assay, DHE is oxidized by $O_2^{\bullet-}$ to ethidium and oxyethidium, producing red fluorescence. This indicator of intracellular $O_2^{\bullet-}$ production was measured by fluorescence spectroscopy and observed by fluorescence microscopy. Briefly, after adenoviral transduction for 48 h, cells were treated with angiotensin II (Ang II; 200 nmol/L) for 20 min. DHE (5 μmol/L) was added to the cells and then incubated for another 20 min at room temperature. Cells were collected, washed, and centrifuged (3000 rpm for 10 min) twice with ice-cold PBS. Cells were then resuspended in 100 μl of PBS, sonicated, and

NIH-PA Author Manuscript

NIH-PA Author Manuscript

NIH-PA Author Manuscript

centrifuged at 5000 rpm for 10 min. The supernatant of each sample was used to measure the amount of protein and to detect fluorescent oxyethidium (excitation/emission at 485 nm/590 nm) in an Optiplate 96 F, using the Synergy HT multimode microplate reader (BioTek Instruments, Winooski, VT, USA) and then normalized to the amount of protein. The experiments were performed three times. The fluorescence intensity was normalized to the control samples without addition of DHE.

Statistical analysis

All data were evaluated with a two-tailed, unpaired Student *t* test or compared by one-way ANOVA followed by Fisher's *t* test and are expressed as means ± SD. A value of $P<0.05$ was considered statistically significant.

Results

SOD2 expression is increased in carotid artery after balloon withdrawal injury

To ascertain the role of SOD2 in vascular remodeling, we first generated a rat carotid artery balloon-injury model and compared SOD2 expression levels in injured arteries with uninjured (control) vessels. Normal and injured arteries at 1, 3, 7, and 14 days after surgery were harvested and paraffin-embedded. Vessel sections were stained with H&E (Fig. 1A, top). Neointima was first observed at 3 days and progressively increased at 7 and 14 days after the injury, as reported previously [16].

To determine the role of SOD2 in neointima formation, SOD2 expression in normal and injured vessels was examined by IHC staining (Fig. 1A, bottom). SOD2 expression was mainly observed in the endothelial cells in the uninjured arteries and its expression was increased in the medial smooth muscle cells in the injured vessels at 1 day after surgery. However, SOD2 expression was decreased in 3 days compared to 1 day after balloon withdrawal injury. Interestingly, SOD2 expression was observed again in neointima at 7 and 14 days after injury. To quantify SOD2 expression after vascular injury, we performed Western blot analysis using proteins extracted from balloon-injured rat carotid arteries at various time points. SOD2 protein expression was upregulated at 1 day, but returned to the baseline 3 days after injury. Consistent with the results of IHC staining, SOD2 expression was upregulated again at 7 and 14 days after balloon injury (Fig. 1B). Quantitative analysis showed that, compared to uninjured vessels, SOD2 protein expression was upregulated by 1.78-fold at 1 day, 2.07-fold at 7 days, and 2.48-fold at 14 days after the injury (Fig. 1C). It appeared that vascular injury caused a biphasic induction of SOD2 expression because 3 days after injury, the SOD2 level was decreased to 0.86-fold of uninjured vessels ($n=3$, $P>0.05$), which was much lower than that at 1 or 7 days after injury. Nevertheless, our data indicate that SOD2 is involved in vascular lesion formation and is probably an important regulator of vascular remodeling.

SOD2 suppresses neointima formation in vivo

To investigate the role of SOD2 in neointimal formation in vivo, recombinant adenoviruses Ad-GFP, Ad-SOD2, and Ad-shSOD2 were generated and prepared. We knocked down or overexpressed SOD2 in the injured vessels via adenovirus-mediated gene transfer. The distal segment of injured left carotid arteries from the proximal edge of the omohyoid muscle to the carotid bifurcation was incubated with saline, Ad-GFP, Ad-SOD2, or Ad-shSOD2 for 20 min immediately after the balloon injury and was harvested 14 days after surgery, followed by fixation, paraffin-embedding, and sectioning. IHC showed no significant change in SOD2 expression between saline-treated and Ad-GFP-transduced vessels. However, SOD2 expression was markedly increased in Ad-SOD2-transduced balloon-injured vessels but was markedly inhibited in Ad-shSOD2-transduced vessels, compared to the saline- or Ad-GFP-

NIH-PA Author Manuscript

NIH-PA Author Manuscript

NIH-PA Author Manuscript

incubated vessels (Fig. 2A, top). These results indicate that exogenously transduced Ad-SOD2 was efficiently expressed, and Ad-shSOD2 successfully blocked SOD2 expression in the neointima in vivo.

Importantly, balloon-injured carotid arteries transduced with Ad-SOD2 exhibited a marked decrease in neointima formation compared with arteries transduced with Ad-GFP (Fig. 2A, middle and bottom). Morphometric analysis of elastic-stained sections showed that over-expression of SOD2 in Ad-SOD2-transduced carotid arteries decreased neointima area by 51% compared to Ad-GFP-transduced vessels (0.075±0.010 versus 0.152±0.021 mm^2; $P<0.01$, $n=6$). Conversely, arteries transduced with Ad-shSOD2 exhibited a significantly thickened neointima compared to those treated with Ad-GFP or saline (Fig. 2B, left). Quantitative analysis showed that SOD2 knockdown increased neointima area by 39% compared to Ad-GFP-transduced vessels (0.211±0.021 versus 0.152±0.021 mm^2; $P<0.05$, $n=6$, Fig. 2B, left). Similar results were obtained when intima/media area ratios were compared (Fig. 2B, right). No significant difference in neointima formation was observed between Ad-GFP- and saline-treated groups (Fig. 2B), consistent with the SOD2 expression (Fig. 2A, top).

SOD2 inhibits VSMC proliferation in vitro

VSMC proliferation plays an important role in neointima formation after vascular injury [16]. To delineate the mechanism by which SOD2 inhibits neointimal formation, we sought to determine whether SOD2 affects VSMC proliferation in vitro. We first evaluated the effect of SOD2 overexpression or knockdown on VSMC proliferation stimulated by 10% FBS. The results showed that SOD2 overexpression inhibited VSMC proliferation and SOD2 knockdown promoted VSMC proliferation compared with Ad-GFP-transduced or nontransduced VSMCs (Fig. 3A). Because Ang II promotes VSMC proliferation through the production of $O_2^{\bullet-}$ [26] and SOD2 scavenges $O_2^{\bullet-}$ [15], we speculated that SOD2 would inhibit, whereas SOD2 knockdown would promote, Ang II-induced VSMC proliferation. Therefore, we determined the effect of SOD2 on Ang II-stimulated VSMC proliferation and found that SOD2 inhibited Ang II-induced cell growth (Fig. 3B), similar to that stimulated by serum. These data demonstrate that SOD2 is a negative modulator for VSMC proliferation.

SOD2 inhibits angiotensin II-induced migration of cultured rat VSMCs

VSMC migration from the media into the intimal surface of blood vessels is an important step during neointima formation after vascular injury [27]. Ang II is a main biologically active agent of the renin–angiotensin system and plays an important role in the migration of VSMCs, which contributes to restenosis after vascular injury [17,26,28]. To explore the mechanisms by which SOD2 inhibits intimal hyperplasia, we used a wound healing assay to evaluate the effect of SOD2 on Ang II-stimulated VSMC migration. As shown in Fig. 4A, Ang II effectively induced VSMC migration (control vs vehicle). SOD2 overexpression, however, inhibited Ang II-induced migration compared with Ad-GFP-treated cells (171±26 versus 236±12 μm; $P<0.05$, $n=6$; Fig. 4B). SOD2 knockdown, on the other hand, promoted Ang II-induced VSMC migration (415±10 versus 236±12 μm; $P<0.01$, $n=6$; Fig. 4B). These data demonstrate that SOD2 suppresses the migration of VSMC stimulated by Ang II.

SOD2 increases the scavenging of superoxide anion in Ang II-stimulated VSMCs

To explore the mechanisms by which SOD2 inhibits Ang II-induced VSMC migration, we evaluated the effect of SOD2 on the scavenging of $O_2^{\bullet-}$ in VSMCs stimulated by Ang II because Ang II-induced VSMC migration and growth are mediated by superoxide generation [26]. We first measured the efficiency of Ad-SOD2 or Ad-shSOD2 in

NIH-PA Author Manuscript

NIH-PA Author Manuscript

NIH-PA Author Manuscript

correspondingly transduced VSMCs by Western blot. We found that SOD2 was highly expressed in Ad-SOD2-transduced VSMCs, whereas SOD2 expression was markedly knocked down in Ad-shSOD2-transduced VSMCs (Fig. 5C). Then, we determined the effect of SOD2 overexpression or knockdown on the scavenging of $O_2^{\bullet-}$ in VSMCs induced by Ang II. As shown in Fig. 5B, SOD2 overexpression effectively scavenged Ang II-induced $O_2^{\bullet-}$ production in VSMCs. However, shRNA knockdown of SOD2 increased $O_2^{\bullet-}$ production (Fig. 5B). The production of $O_2^{\bullet-}$ was 0.43-fold in Ad-SOD2-transduced VSMCs (n=3, P<0.01) and 3.55-fold in Ad-shSOD2-transduced VSMCs (n=3, P<0.01), compared to Ad-GFP-transduced VSMCs (Fig. 5B). No significant difference was observed between Ad-GFP-transduced VSMCs and nontransduced VSMCs (control; n=3, P>0.05; Fig. 5B). These data suggest that SOD2 plays an important role in scavenging Ang II-induced $O_2^{\bullet-}$ in VSMCs.

SOD2 inhibits Ang II-stimulated VSMC migration through attenuation of Akt phosphorylation

Previous studies have shown that Ang II-induced migration of choriocarcinoma cells is mediated by the phosphatidylinositol 3-kinase (PI3K)/Akt signaling pathway [29]. Activation of Akt also plays an important role in Ang II-induced proliferation of rat aortic SMCs and CHO cells stably expressing the rat AT1A receptor [30]. However, it remains unknown if Akt phosphorylation is involved in Ang II-induced VSMC migration. We first investigated if Ang II induces Akt phosphorylation in VSMCs and then explored the role of SOD2 in the Akt phosphorylation and VSMC migration. We found that Ang II promoted the phosphorylation of Akt in VSMCs. SOD2 overexpression markedly inhibited the Ang II-induced Akt phosphorylation, whereas SOD2 knockdown significantly enhanced the phosphorylation (Fig. 6A). To determine if activation of Akt is involved in SOD2 regulation of VSMC migration, we evaluated whether a PI3K-specific inhibitor, LY294002, alters the effect of SOD2 on Ang II-induced VSMC migration. We found that shRNA knockdown of SOD2 enhanced Akt phosphorylation, which was blocked by LY294002, suggesting that SOD2 inhibited Akt activation through PI3K (Fig. 6B). Moreover, PI3K inhibitor reversed the effect of SOD2 knockdown on Ang II-induced VSMC migration (Fig. 6C). Taken together, our data suggest that the effect of SOD2 on VSMC migration was exerted, at least in part, through modulation of the PI3K/Akt signaling pathway.

Discussion

SOD2 is a unique form of superoxide dismutase containing manganese and is located in the mitochondria, the most important sources of $O_2^{\bullet-}$ [15]. Because of its special subcellular localization, SOD2 is of considered to be the first line of defense against oxidative stress and plays a central role in metabolizing superoxide [11]. $O_2^{\bullet-}$ plays an important role in neointima formation and is essential for neointimal VSMC proliferation [5]. To gain an insight into the role of SOD2 in neointima formation after vascular injury, we examined the effects of SOD2 on neointima formation in rat balloon-injured carotid artery and observed its effects on Ang II-induced rat aortic smooth muscle cell proliferation and migration. This study demonstrates for the first time that SOD2 is increased along with the development of neointima after balloon-withdrawal injury. Importantly, SOD2 overexpression inhibited, whereas SOD2 knockdown promoted, the neointima formation. These findings demonstrate that SOD2 is a novel negative modulator in neointima formation after vascular injury.

It is intriguing that SOD2 expression exhibited a biphasic pattern after vascular injury and in the process of remodeling. SOD2 was activated immediately after the injury (1 day postinjury), and then its expression returned to the baseline. Seven days later, SOD2 was gradually activated again and was highly expressed in the neointimal area 14 days after

NIH-PA Author Manuscript

NIH-PA Author Manuscript

NIH-PA Author Manuscript

injury. The initial burst of SOD2 that occurred in the media layer was probably a spontaneous response of the vessel to the $O_2^{\bullet-}$ induced by the injury. The initial SOD2 upregulation vanished after the early stress. The later inflammatory response following the mechanical injury caused the production of $O_2^{\bullet-}$ in the vascular wall, resulting in the neointima formation. The second burst of SOD2 was a response of the vessel to $O_2^{\bullet-}$ produced in the neointima, aimed at limiting the thickening of the vessel wall. SOD2 was unable to completely halt the growth of neointima because the endogenous level of SOD2 was not sufficient, and more importantly, other factors were also promoting the neointima formation.

VSMC migration and proliferation play major roles in vascular remodeling [3]. Ang II-induced VSMC migration and growth in vascular remodeling is mediated by superoxide generation [26]. To elucidate the mechanisms by which SOD2 regulates neointima formation, we explored the effect of SOD2 on VSMC migration and proliferation induced by Ang II. SOD2 overexpression significantly inhibited, whereas SOD2 knockdown promoted, Ang II-induced VSMC migration and proliferation. The effect of SOD2 on VSMC proliferation is consistent with a previous report showing that SOD2 overexpression in fawn-hooded rat pulmonary artery smooth muscle cells or therapy with the SOD2 mimetic MnTBAP reverses the hyperproliferative phenotype in pulmonary artery hypertension [31]. Our studies indicate that SOD2 inhibits neointima formation via attenuation of both VSMC proliferation and migration. SOD2 seems to inhibit VSMC migration and proliferation by scavenging $O_2^{\bullet-}$ that can be induced by Ang II. Overexpression of SOD2 significantly enhanced, whereas SOD2 knockdown decreased, the scavenging of $O_2^{\bullet-}$.

It has been reported that PI3K/Akt signaling is involved in the Ang II-induced VSMC proliferation [30]. However, it is unknown whether the PI3K/Akt pathway plays a role in Ang II-induced VSMC migration. In this study, we found that SOD2 overexpression inhibited, whereas SOD2 knockdown enhanced, Ang II-induced Akt phosphorylation. A specific inhibitor of PI3 kinase, LY294002, abolished the effect of SOD2 knockdown on Ang II-induced Akt phosphorylation, suggesting that SOD2 regulated Akt phosphorylation by modulating PI3K activity, consistent with a previous report showing that reactive oxygen species activate PI3K [32]. Importantly, the effect of SOD2 knockdown on Ang II-induced VSMC migration was blocked by the PI3K inhibitor, indicating that SOD2 inhibits Ang II-induced VSMC migration through attenuation of PI3K/Akt signaling. These results demonstrate that vascular injury induces $O_2^{\bullet-}$ production via Ang II, which activates PI3K/Akt signaling, leading to SMC migration. SOD2 inhibits $O_2^{\bullet-}$ production and this prevents the SMC migration.

PI3K is cytosolic protein and interacts with cell membranes, and mitochondrial SOD2 modulates PI3K/Akt signaling. It is interesting that these distinctly compartmentalized proteins can interact with each other to influence SMC migration and proliferation during vascular remodeling. It is possible that $O_2^{\bullet-}$ produced in mitochondria diffuses into the cytoplasm to activate PI3K. SOD2 scavenges mitochondrial $O_2^{\bullet-}$, and thus inhibits PI3K activation. Alternatively, SOD2 may affect PI3K activity through nanocontacts between cell membrane and mitochondria. A previous study has shown that membrane structures called caveolae in vascular SMCs have nanocontacts with mitochondria [33]. Although these contacts involve only a small percentage (10%) of caveolae, they may be sufficient for the structural support needed for the interaction between SOD2/ROS and PI3K signaling.

Taken together, the results of this study have identified SOD2 as a negative mediator for vascular lesion formation in experimental angioplasty. SOD2 inhibits vascular remodeling

NIH-PA Author Manuscript

NIH-PA Author Manuscript

NIH-PA Author Manuscript

by attenuating VSMC migration and proliferation, which is mediated by the scavenging of $O_2^{\bullet -}$ and regulation of PI3K/Akt signaling. Our results indicate that SOD2 augmentation may represent a promising therapeutic strategy for the prevention of restenosis after percutaneous coronary intervention.

Acknowledgments

This work was supported by grants from the National Institutes of Health (HL093429 and HL107526 to Dr. Chen).

References

1. Joner M, Finn AV, Farb A, Mont EK, Kolodgie FD, Ladich E, Kutys R, Skorija K, Gold HK, Virmani R. Pathology of drug-eluting stents in humans: delayed healing and late thrombotic risk. J Am Coll Cardiol. 2006; 48:193–202. [PubMed: 16814667]
2. Chatterjee S, Pandey A. Drug eluting stents: friend or foe? A review of cellular mechanisms behind the effects of Paclitaxel and sirolimus eluting stents. Curr Drug Metab. 2008; 9:554–566. [PubMed: 18680476]
3. Ross R. The pathogenesis of atherosclerosis: a perspective for the 1990s. Nature. 1993; 362:801–809. [PubMed: 8479518]
4. Lowe HC, Oesterle SN, Khachigian LM. Coronary in-stent restenosis: current status and future strategies. J Am Coll Cardiol. 2002; 39:183–193. [PubMed: 11788206]
5. Kanellakis P, Nestel P, Bobik A. Angioplasty-induced superoxide anions and neointimal hyperplasia in the rabbit carotid artery: suppression by the isoflavone trans-tetrahydrodaidzein. Atherosclerosis. 2004; 176:63–72. [PubMed: 15306176]
6. Matesanz N, Lafuente N, Azcutia V, Martin D, Cuadrado A, Nevado J, Rodriguez-Manas L, Sanchez-Ferrer CF, Peiro C. Xanthine oxidase-derived extracellular superoxide anions stimulate activator protein 1 activity and hypertrophy in human vascular smooth muscle via c-Jun N-terminal kinase and p38 mitogen-activated protein kinases. J Hypertens. 2007; 25:609–618. [PubMed: 17278978]
7. Callsen D, Sandau KB, Brune B. Nitric oxide and superoxide inhibit platelet-derived growth factor receptor phosphotyrosine phosphatases. Free Radic Biol Med. 1999; 26:1544–1553. [PubMed: 10401621]
8. Kanellakis P, Pomilio G, Walker C, Husband A, Huang JL, Nestel P, Agrotis A, Bobik A. A novel antioxidant 3,7-dihydroxy-isoflav-3-ene (DHIF) inhibits neointimal hyperplasia after vessel injury attenuating reactive oxygen species and nuclear factor-kappaB signaling. Atherosclerosis. 2009; 204:66–72. [PubMed: 18930230]
9. Madamanchi NR, Moon SK, Hakim ZS, Clark S, Mehrizi A, Patterson C, Runge MS. Differential activation of mitogenic signaling pathways in aortic smooth muscle cells deficient in superoxide dismutase isoforms. Arterioscler Thromb Vasc Biol. 2005; 25:950–956. [PubMed: 15746439]
10. Mendez JI, Nicholson WJ, Taylor WR. SOD isoforms and signaling in blood vessels: evidence for the importance of ROS compartmentalization. Arterioscler Thromb Vasc Biol. 2005; 25:887–888. [PubMed: 15863719]
11. Faraci FM, Didion SP. Vascular protection: superoxide dismutase isoforms in the vessel wall. Arterioscler Thromb Vasc Biol. 2004; 24:1367–1373. [PubMed: 15166009]
12. Laukkanen MO, Kivela A, Rissanen T, Rutanen J, Karkkainen MK, Leppanen O, Brasen JH, Yla-Herttuala S. Adenovirus-mediated extracellular superoxide dismutase gene therapy reduces neointima formation in balloon-denuded rabbit aorta. Circulation. 2002; 106:1999–2003. [PubMed: 12370226]
13. Durand E, Al Haj Zen A, Addad F, Brasselet C, Caligiuri G, Vinchon F, Lemarchand P, Desnos M, Bruneval P, Lafont A. Adenovirus-mediated gene transfer of superoxide dismutase and catalase decreases restenosis after balloon angioplasty. J Vasc Res. 2005; 42:255–265. [PubMed: 15870505]
14. Brasen JH, Leppanen O, Inkala M, Heikura T, Levin M, Ahrens F, Rutanen J, Pietsch H, Bergqvist D, Levonen AL, Basu S, Zeller T, Kloppel G, Laukkanen MO, Yla-Herttuala S. Extracellular

NIH-PA Author Manuscript

NIH-PA Author Manuscript

NIH-PA Author Manuscript

superoxide dismutase accelerates endothelial recovery and inhibits in-stent restenosis in stented atherosclerotic Watanabe heritable hyperlipidemic rabbit aorta. J Am Coll Cardiol. 2007; 50:2249–2253. [PubMed: 18061074]

15. Dikalova AE, Bikineyeva AT, Budzyn K, Nazarewicz RR, McCann L, Lewis W, Harrison DG, Dikalov SI. Therapeutic targeting of mitochondrial superoxide in hypertension. Circ Res. 2010; 107:106–116. [PubMed: 20448215]
16. Wang JN, Shi N, Xie WB, Guo X, Chen SY. Response gene to complement 32 promotes vascular lesion formation through stimulation of smooth muscle cell proliferation and migration. Arterioscler Thromb Vasc Biol. 2011; 31:e19–26. [PubMed: 21636805]
17. Zhang F, Hu Y, Xu Q, Ye S. Different effects of angiotensin II and angiotensin-(1–7) on vascular smooth muscle cell proliferation and migration. PLoS One. 2010; 5:e12323. [PubMed: 20808802]
18. Clowes AW, Reidy MA, Clowes MM. Mechanisms of stenosis after arterial injury. Lab Invest. 1983; 49:208–215. [PubMed: 6876748]
19. Dollery CM, McEwan JR. Local gene delivery of recombinant adenoviruses to the rat carotid artery in vivo. Methods Mol Med. 1999; 30:417–435. [PubMed: 21341044]
20. Tulis DA. Histological and morphometric analyses for rat carotid balloon injury model. Methods Mol Med. 2007; 139:31–66. [PubMed: 18287663]
21. Tulis DA. Rat carotid artery balloon injury model. Methods Mol Med. 2007; 139:1–30. [PubMed: 18287662]
22. Xie WB, Li Z, Miano JM, Long X, Chen SY. Smad3-mediated myocardin silencing: a novel mechanism governing the initiation of smooth muscle differentiation. J Biol Chem. 2011; 286:15050–15057. [PubMed: 21402709]
23. Loo AE, Ho R, Halliwell B. Mechanism of hydrogen peroxide-induced kerati-nocyte migration in a scratch-wound model. Free Radic Biol Med. 2011; 51:884–892. [PubMed: 21699973]
24. Tang JM, Wang JN, Zhang L, Zheng F, Yang JY, Kong X, Guo LY, Chen L, Huang YZ, Wan Y, Chen SY. VEGF/SDF-1 promotes cardiac stem cell mobilization and myocardial repair in the infarcted heart. Cardiovasc Res. 2011; 91:402–411. [PubMed: 21345805]
25. Yang D, Tan Z, Pan JY, Wang TH. 17beta-Estradiol inhibits vascular smooth muscle cell proliferation and c-fos expression: role of nitric oxide. Sheng Li Xue Bao. 2002; 54:17–22. [PubMed: 11930235]
26. Yaghini FA, Song CY, Lavrentyev EN, Ghafoor HU, Fang XR, Estes AM, Campbell WB, Malik KU. Angiotensin II-induced vascular smooth muscle cell migration and growth are mediated by cytochrome P450 1B1-dependent superoxide generation. Hypertension. 2010; 55:1461–1467. [PubMed: 20439821]
27. Hao H, Gabbiani G, Bochaton-Piallat ML. Arterial smooth muscle cell heterogeneity: implications for atherosclerosis and restenosis development. Arterioscler Thromb Vasc Biol. 2003; 23:1510–1520. [PubMed: 12907463]
28. Allen CL, Bayraktutan U. Differential mechanisms of angiotensin II and PDGF-BB on migration and proliferation of coronary artery smooth muscle cells. J Mol Cell Cardiol. 2008; 45:198–208. [PubMed: 18573259]
29. Ishimatsu S, Itakura A, Okada M, Kotani T, Iwase A, Kajiyama H, Ino K, Kikkawa F. Angiotensin II augmented migration and invasion of choriocarcino-ma cells involves PI3K activation through the AT1 receptor. Placenta. 2006; 27:587–591. [PubMed: 16122787]
30. Dugourd C, Gervais M, Corvol P, Monnot C. Akt is a major downstream target of PI3-kinase involved in angiotensin II-induced proliferation. Hypertension. 2003; 41:882–890. [PubMed: 12623864]
31. Archer SL, Marsboom G, Kim GH, Zhang HJ, Toth PT, Svensson EC, Dyck JR, Gomberg-Maitland M, Thebaud B, Husain AN, Cipriani N, Rehman J. Epigenetic attenuation of mitochondrial superoxide dismutase 2 in pulmonary arterial hypertension: a basis for excessive cell proliferation and a new therapeutic target. Circulation. 2010; 121:2661–2671. [PubMed: 20529999]
32. Ndiaye M, Chataigneau M, Lobysheva I, Chataigneau T, Schini-Kerth VB. Red wine polyphenol-induced, endothelium-dependent NO-mediated relaxation is due to the redox-sensitive PI3-kinase/

NIH-PA Author Manuscript

NIH-PA Author Manuscript

NIH-PA Author Manuscript

Akt-dependent phosphorylation of endothelial NO-synthase in the isolated porcine coronary artery. FASEB J. 2005; 19:455–457. [PubMed: 15623569]

33. Popescu LM, Gherghiceanu M, Mandache E, Cretoiu D. Caveolae in smooth muscles: nanocontacts. J Cell Mol Med. 2006; 10:960–990. [PubMed: 17125599]

NIH-PA Author Manuscript

NIH-PA Author Manuscript

NIH-PA Author Manuscript

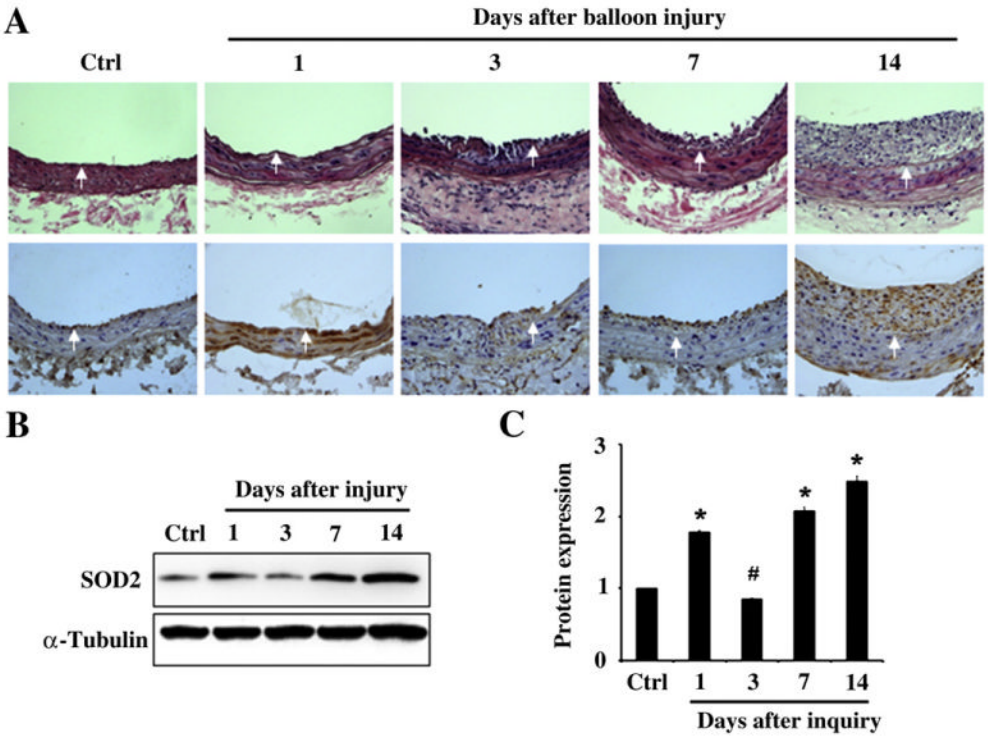

Fig. 1.

Expression of SOD2 in balloon-injured carotid artery. (A) Top: H&E staining of carotid artery sections. Paraffin-embedded sections prepared from uninjured (Ctrl) or balloon-injured carotid arteries at 1, 3, 7, and 14 days after surgery were stained with H&E. Neointima formations shown at various time points are representative of three independent experiments. Arrows indicate internal elastic lamina. Original magnification was 200×. Bottom: SOD2 expression by IHC. The carotid artery sections were incubated with mouse anti-SOD2 monoclonal antibody followed by HRP-conjugated goat anti-mouse secondary antibody and DAB staining. Original magnification was 200×. (B) Western blot of SOD2 protein in injured carotid arteries. Artery proteins were extracted from control and balloon-injured rat carotid arteries at various time points as indicated. Samples were probed with anti-SOD2 monoclonal antibody (1:1000 diluted). α-Tubulin served as an internal control. Three independent experiments were performed. (C) Relative SOD2 expression levels were quantified by ImageJ software. $^{*}P<0.01$, $^{\#}P>0.05$ compared with Ctrl group, $n=3$.

NIH-PA Author Manuscript

NIH-PA Author Manuscript

NIH-PA Author Manuscript

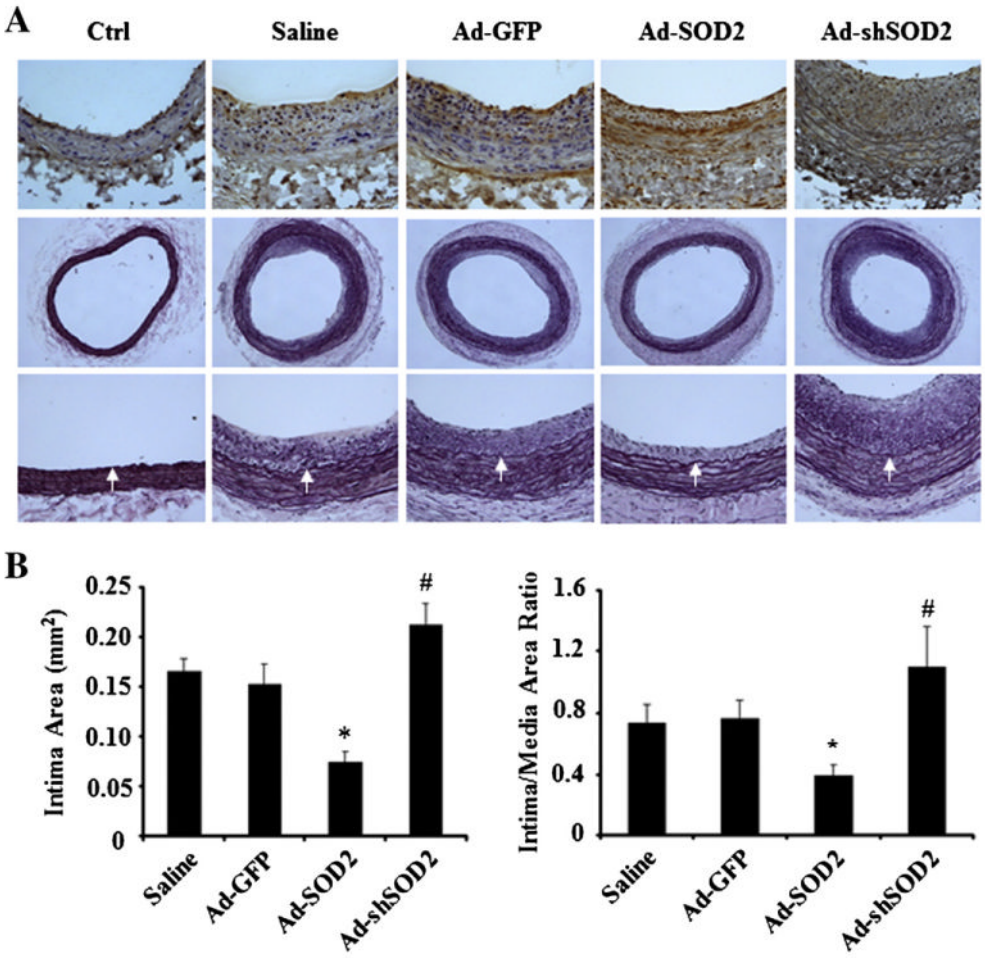

Fig. 2.

Effect of SOD2 on neointima formation in rat balloon-injured carotid arteries. (A) Top: SOD2 expression in rat balloon-injured carotid arteries transduced with Ad-GFP, Ad-SOD2, or Ad-shSOD2. Uninjured normal (Ctrl) or 14-day injured carotid arteries incubated with 0.9% saline or Ad-GFP, Ad-SOD2, or Ad-shSOD2 for 20 min were harvested, fixed, embedded, and sectioned. The sections were incubated with mouse anti-SOD2 monoclonal antibody followed by HRP-conjugated goat anti-mouse secondary antibody and DAB staining. Original magnification was 200×. Middle and bottom: Representative photomicrographs of balloon-injured, perfusion-fixed, Elastica van Gieson-stained carotid artery cross sections at day 14. Arrows indicate internal elastic lamina. Middle row original magnification was 40×; bottom row original magnification was 200×. (B) Quantitative analysis of intima area (left) and intima/media ratio (right). Results are expressed as means ±SD. $^{*}P<0.01$, $^{\#}P<0.05$ compared with saline- or Ad-GFP-treated arteries, $n=6$.

NIH-PA Author Manuscript

NIH-PA Author Manuscript

NIH-PA Author Manuscript

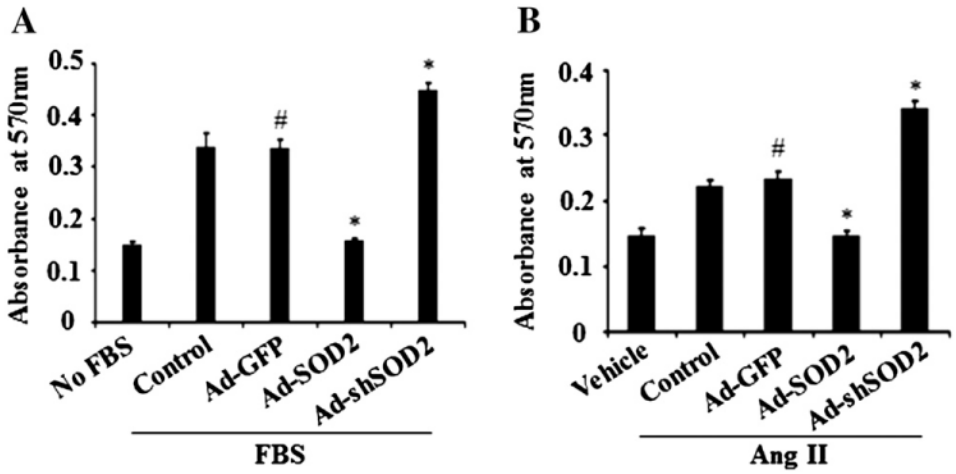

Fig. 3.

Effect of SOD2 on serum- or Ang II-induced VSMC proliferation. (A) SOD2 overexpression inhibited serum-stimulated VSMC proliferation. VSMCs were transduced with adenoviruses as indicated for 48 h. The cells were then trypsinized, seeded onto 96-well plates, and cultured in medium containing 10% FBS. 48 h later, MTT assay was performed. Data are expressed as means±SD. *P <0.01 compared with control or Ad-GFP group, $^{\#}P$ >0.05 compared with control group, n =6. (B) SOD2 overexpression inhibited Ang II-induced VSMC proliferation. VSMCs were infected with Ad-GFP or Ad-SOD2 or Ad-shSOD2 and serum-starved 24 h. Cells were then exposed to vehicle or Ang II (200 nM) for 24 h as indicated. MTT assay was performed. Data are expressed as means±SD. *P <0.01 compared to control or Ad-GFP group, #P >0.05 compared to control group, n =6.

NIH-PA Author Manuscript

NIH-PA Author Manuscript

NIH-PA Author Manuscript

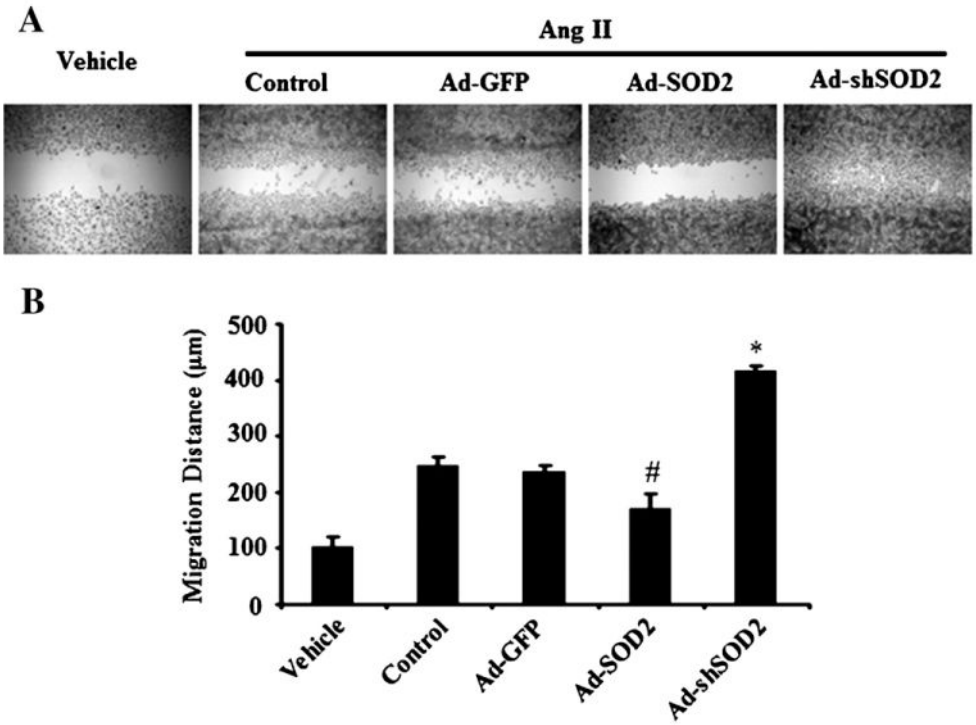

Fig. 4.

Effect of SOD2 on Ang II-induced VSMC migration. (A) Representative microphotographs of wound healing assay of VSMCs transduced with Ad-GFP, Ad-SOD2, or Ad-shSOD2. VSMCs infected with the indicated adenoviruses were seeded onto fibronectin-coated 24-well cell culture plates containing a wound healing insert with a width of 0.9 mm and incubated for 24 h, followed by carefully removing the insert from the well to begin the wound healing assay. The cells were treated with vehicle or Ang II (200 nM) for 48 h. Cells were fixed and stained with cell stain solution. Pictures were taken on a dissection microscope at a magnification of 40×. (B) Quantitative analysis of the migration distance. $^{*}P<0.01$, $^{\#}P>0.05$ compared with Ad-GFP or control group, $n=6$.

NIH-PA Author Manuscript

NIH-PA Author Manuscript

NIH-PA Author Manuscript

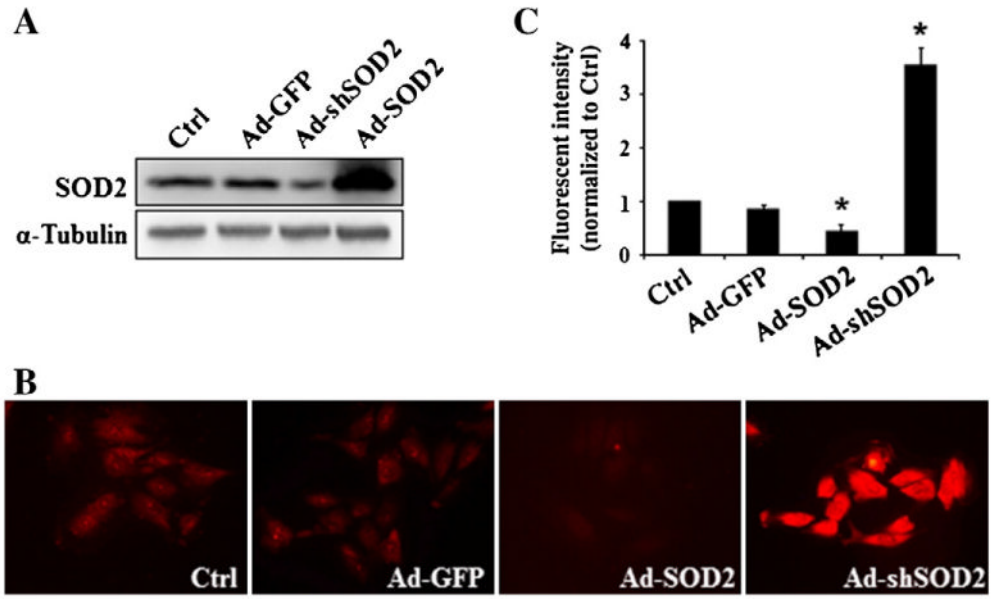

Fig. 5.

SOD2 scavenges superoxide anion in VSMCs. (A) Representative fluorescence microphotographs showing intracellular superoxide production in VSMCs stimulated with Ang II. VSMCs were transduced with Ad-GFP, Ad-SOD2, or Ad-shSOD2 or left untreated (Ctrl) for 48 h. The cells were then exposed to Ang II (200 nM) for 20 min and then were incubated with dihydroethidium (5 μM) for an additional 20 min. The cells were washed with PBS three times and fixed with methanol:acetic acid (1:1). Fluorescent oxyethidium, an indicator of intracellular superoxide production, was observed with fluorescence microscopy. (B) Quantitative analysis of intracellular superoxide production in Ang II-stimulated VSMCs. Cells were treated as described for (A). Oxyethidium-produced red fluorescence was measured with fluorescence spectroscopy and normalized to protein concentration. The fluorescence intensity in the Ctrl group was arbitrarily defined as 1. The values of three experiments are shown as means±SD. *P<0.01 compared with Ad-GFP or control group. (C) Levels of SOD2 expression in VSMCs infected with Ad-GFP, Ad-shSOD2, or Ad-SOD2 were analyzed by Western blot.

NIH-PA Author Manuscript

NIH-PA Author Manuscript

NIH-PA Author Manuscript

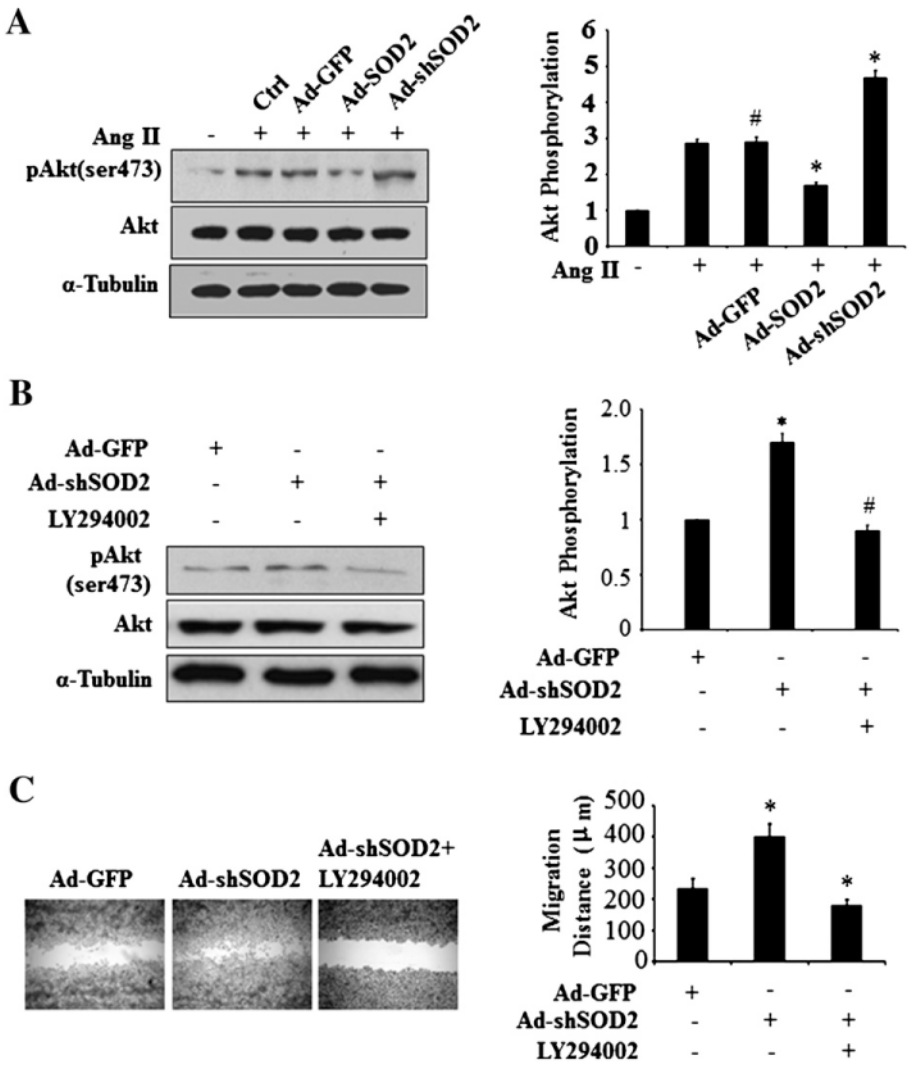

Fig. 6.

SOD2 regulates Akt phosphorylation in VSMC migration. (A) SOD2 overexpression inhibited Ang II-induced phosphorylation. VSMCs were transduced with Ad-GFP, Ad-SOD2, or Ad-shSOD2 or left untreated (Ctrl) for 48 h and then exposed to vehicle (−) or Ang II (200 nM) for 30 min. Protein samples were extracted and blotted with antibodies against phospho-Akt (pAkt (Ser473)), Akt, or α-tubulin. Left: Western blot of Akt phosphorylation. Right: quantitative analysis of Akt phosphorylation level. The Akt phosphorylation level in VSMCs treated with vehicle (−) was arbitrarily defined as 1. Values are the means±SD of three different sets of experiments. *P<0.01 compared to Ad-GFP, #P>0.05 compared to Ang II-treated cells without adenovirus transduction (+). (B) SOD2 regulates Akt phosphorylation via PI3K. VSMCs were transduced with Ad-GFP or Ad-shSOD2 for 48 h and stimulated with Ang II with or without the PI3K inhibitor LY294002 (10 μM) for 30 min as indicated. Proteins samples were probed with antibodies against phospho-Akt (Ser473), Akt, and α-tubulin. Left: representative blots showing that PI3K inhibitor reversed the effect of SOD2 knockdown on Akt phosphorylation. Right: quantitative analysis of Akt phosphorylation level. Akt phosphorylation level in VSMCs transduced with Ad-GFP was arbitrarily defined as 1. Values shown are the means±SD from three independent experiments. *P<0.01, #P>0.05 compared with Ad-GFP group. (C) The

NIH-PA Author Manuscript

NIH-PA Author Manuscript

NIH-PA Author Manuscript

PI3K inhibitor LY294002 reversed the effect of SOD2 knockdown on VSMC migration. Left: representative microphotographs of VSMC migration. PI3K inhibitor blocked VSMC migration enhanced by SOD2 knockdown. Right: quantitative analysis of VSMC migration distance demonstrates that SOD2 knockdown-mediated migration was inhibited by PI3K inhibitor. *P<0.01 compared with Ad-GFP group, n=6.